

Figure 7 Simulation and measurement results of the proposed filter. [Color figure can be viewed in the online issue, which is available at wileyonlinelibrary.com]

the range of 2.7–6.6 GHz. Owing to the two transmission zeros in the lower and upper cut-off frequencies, sharp selectivity is observed. Besides, a transmission zero due to the source-load coupling is generated at 8.76 GHz and improves the stopband performance. The measured upper stopband with 25 dB attenuation level is extended to 11.4 GHz. The minimum and maximum insertion loss with the frequency range 2.9–6.28 GHz is 0.24 and 0.64 dB, respectively, and the measured return loss is better than 10.8 dB against its counterpart of 13.3 dB in simulation, where the discrepancy may be due to the unexpected tolerance of fabrication and implement. In addition, the group delay within the passband is between 0.30 and 0.66 ns, and the low group delay variation (0.36 ns) shows a good linearity.

4. CONCLUSION

This article presents a tri-mode wideband BPF. By using the shunted short- and open-stub loaded resonators, three independent modes can be combined within the passband, and the lower and upper passband bandwidths can be independently controlled. Besides, sharp passband selectivity can be obtained by the transmission zeros at the lower and upper cut-off frequencies. Simulated and measured results show that the proposed filter has the advantages of low insertion loss, sharp passband selectivity, good stopband performance as well as flexible design and optimize process.

ACKNOWLEDGMENT

This work is supported by the National Natural Science Foundation of China (61171029 and 61101016).

REFERENCES

1. L. Zhu, S. Sun, and W. Menzel, Ultra-wideband (UWB) bandpass filters using multiple-mode resonator, *IEEE Microw Wirel Compon Lett* 15 (2005), 796–798.
2. S.W. Wong and L. Zhu, Quadruple-mode UWB bandpass filter with improved out-of-band rejection, *IEEE Microw Wirel Compon Lett* 19 (2009), 152–154.
3. Q.X. Chu and X.K. Tian, Design of UWB bandpass filter using stepped-impedance stub-loaded resonator, *IEEE Microw Wirel Compon Lett* 20 (2010), 501–503.
4. H. Wang, Q.X. Chu, and J.Q. Gong, A compact wideband microstrip filter using folded multiple-mode resonator, *IEEE Microw Wirel Compon Lett* 19 (2009), 287–289.
5. M. Nosrati and M. Mirzaee, Compact wideband microstrip bandpass filter using quasi-spiral loaded multiple-mode resonator, *IEEE Microw Wirel Compon Lett* 20 (2010), 607–609.

6. Q.X. Chu, F.C. Chen, and H. Wang, A novel crossed resonator and its applications to bandpass filters, *IEEE Trans Microw Theory Tech* 57 (2009), 1753–1759.
7. L. Han, K. Wu, and X.P. Zhang, Development of packaged ultra-wideband bandpass filters, *IEEE Trans Microw Theory Tech* 58 (2010), 220–228.
8. K.J. Song and Q. Xue, Novel broadband bandpass filters using Y-shaped dual-mode microstrip resonators, *IEEE Microw Wirel Compon Lett* 19 (2009), 548–550.
9. L. Zhu and W. Menzel, Compact microstrip bandpass filter with two transmission zeros using a stub-tapped half-wavelength line resonator, *IEEE Microw Wirel Compon Lett* 13 (2003), 16–18.
10. W. Shen, X.W. Sun, and W.Y. Yin, A novel microstrip filter using three-mode stepped impedance resonator (TSIR), *IEEE Microw Wirel Compon Lett* 19 (2009), 774–776.
11. F.C. Chen, Q.X. Chu, and Z.H. Tu, Design of compact dual-band bandpass filter using short stub loaded resonator, *Microw Opt Technol Lett* 51 (2009), 1238–1240.
12. X.Y. Zhang, J.X. Chen, Q. Xue, and S.M. Li, Dual-band bandpass filters using stub-loaded resonators, *IEEE Microw Wirel Compon Lett* 17 (2007), 583–585.

© 2013 Wiley Periodicals, Inc.

STRIPLINE BANDPASS FILTER WITH WIDE STOPBAND AND REJECTION LEVEL UP TO 100 dB

B.A. Belyaev,¹ A.M. Serzhantov,² V.V. Tyurnev,¹ A.A. Leksikov,¹ and Y.F. Bal'va³

¹Kirensky Institute of Physics, Siberian Branch, Russian Academy of Sciences, Krasnoyarsk, Russia; Corresponding author: belyaev@iph.krasn.ru

²Institute of Engineering Physics and Radio Electronics, Siberian Federal University, Krasnoyarsk, Russia

³Reshetnev Siberian State Aerospace University, Krasnoyarsk, Russia

Received 8 April 2013

ABSTRACT: A novel miniature stripline resonator performed on a double-layer suspended substrate and bandpass filters (BPFs) based on it are proposed. The filters have wide stopband with high attenuation. A fifth-order BPF has been designed and fabricated. The filter stopband at level of -100 dB extends up to the frequency that exceeds the passband center frequency by factor of 10. It is shown that miniature filters based on the proposed resonator could be effectively fabricated by low temperature cofired ceramics technology. © 2013 Wiley Periodicals, Inc. *Microw Opt Technol Lett* 55:2866–2869, 2013; View this article online at wileyonlinelibrary.com. DOI 10.1002/mop.28013

Key words: BPF; suspended stripline resonator; double-layer substrate; wide stopband; LTCC

1. INTRODUCTION

Miniature bandpass filters (BPFs) are important elements of modern microwave wireless communication systems. Filters having wide stopband with high attenuation level are required for effective interference suppression.

One of widespread methods for stopband widening is usage of stepped impedance resonators in which the fundamental mode frequency may be significantly lower than the frequency of the lowest high-order mode. Stopband width in such BPFs increases with increase of the impedance step [1,2]. However, this widening is accompanied by significant decay of resonator unloaded Q factor due to the rise of ohmic loss in the narrow strip conductor. For suppression the lowest spurious passband, dissimilar stepped impedance

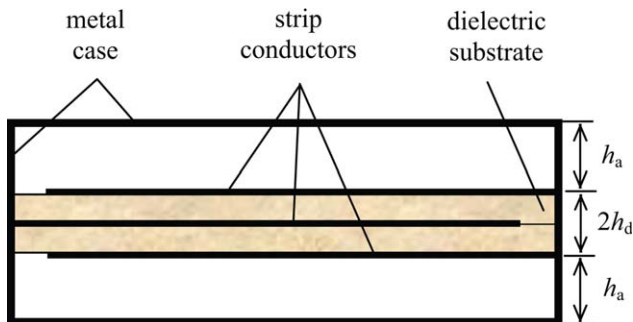


Figure 1 Longitudinal section of the suspended stripline resonator. [Color figure can be viewed in the online issue, which is available at wileyonlinelibrary.com]

resonators with differing frequencies of high-order modes may be used in a filter [3]. In order to suppress one of spurious passbands, it is often proposed to use transmission zeros that arise when the input and output resonators are tapped to the filter ports [4–6]. One more way to widen the stopband width is nullification of the coupling between some adjacent resonators at one of high-order mode frequencies [5,6]. That is possible while mutual compensation of the inductive and capacitive interactions between the resonators which may occur, for example, for specific coupling length [7–9].

Although, a certain progress in development of BPFs with wide stopband has been achieved, the upper edge of the stopband at level of -60 dB in all cited papers does not exceed $8f_0$, where f_0 is the passband center frequency. One of ways of further widening the stopband lies through developing new structures of resonators whose the second mode frequency many times exceeds the first mode frequency. For example, a fourth-order BPF based on novel coaxial resonators [10] has the upper stopband at the level of -90 dB which extends up to $47f_0$ [11]. However, from point of view of manufacturability, reliability, and cost such BPFs are significantly worse than constructions based on stripline or microstrip structures.

In this article, we offer the novel construction of miniature stripline resonator which allows designing BPFs with extremely deep and wide stopband.

2. MINIATURE SUSPENDED STRIPLINE RESONATOR

The resonator (Fig. 1) consists of a double-layer suspended substrate with three strip conductors placed one under another. Two outer conductors are connected by one of their ends to one of the sidewalls of the metal shielding case. The third (inner) conductor is connected by one of its ends to the opposite sidewall.

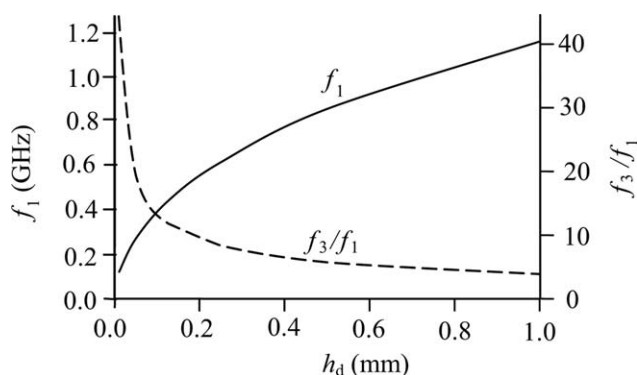


Figure 2 The first mode frequency and the frequency ratio of the third and the first mode as functions of the dielectric layer thickness

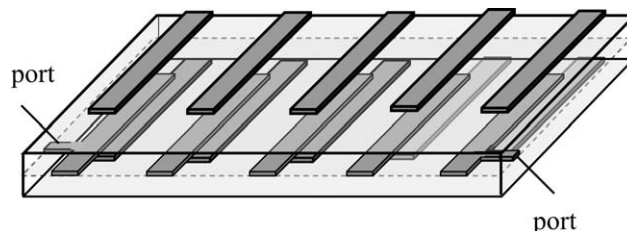


Figure 3 The suspended stripline filter (the metal case is not shown)

All other ends of the strip conductors do not stretch to the sidewalls and remain open circuited.

The first oscillation mode has the lowest frequency f_1 . This mode is selected as an operating oscillation mode. The currents in all three conductors of the first mode flow in the same direction. The second mode has the higher frequency f_2 . The currents of the second mode flow in the upper and lower conductors in opposite directions and the current in the inner conductor does not flow. The frequency of the third mode f_3 is higher than f_2 . The currents of the third mode flow in the upper and lower conductors in the same direction and the current in the inner conductor flows in the opposite direction.

It is important to note that excitation of the second mode in the resonators of BPFs can be hindered if the input and output resonators are coupled with the filter ports by the use of taps situated on the inner strip conductors. In this case, the lowest spurious bandpass is due to the third oscillation mode. Then the bandwidth of the stopband is determined by the ratio f_3/f_1 .

Our study shows that a structure parameter having the greatest influence on f_1 and f_3/f_1 is the thickness of the substrate layer h_d . Two dependences presented in Figure 2 were obtained by electromagnetic 3D simulation with use of Ansoft HFSS. In the simulation, the following parameters were used: resonator length $l_r = 20$ mm, length of the strip conductor $l_s = 0.98l_r$, conductor width $w = 3$ mm, height of the air gaps $h_a = 3.5$ mm, permittivity of the substrate layers $\epsilon_r = 2.2$.

One can see that with decrease in thickness h_d the frequency f_1 drops and the ratio f_3/f_1 grows. Note that increase in f_3/f_1 is accompanied by significant decrease in the resonator length l_r and insignificant increase in Q factor when f_1 is fixed. Decrease in ohmic loss in the last dependence is due to shortening the conductor length l_s .

An additional increase in the stopband width may be obtained by widening the strip width w and increasing the height h_a . However that results in enlargement of the filter size. Increase in permittivity ϵ_r insignificantly widens the stopband width too.

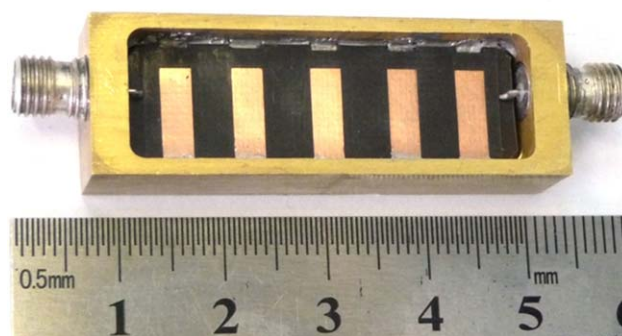


Figure 4 Photograph of the fabricated suspended stripline filter. [Color figure can be viewed in the online issue, which is available at wileyonlinelibrary.com]

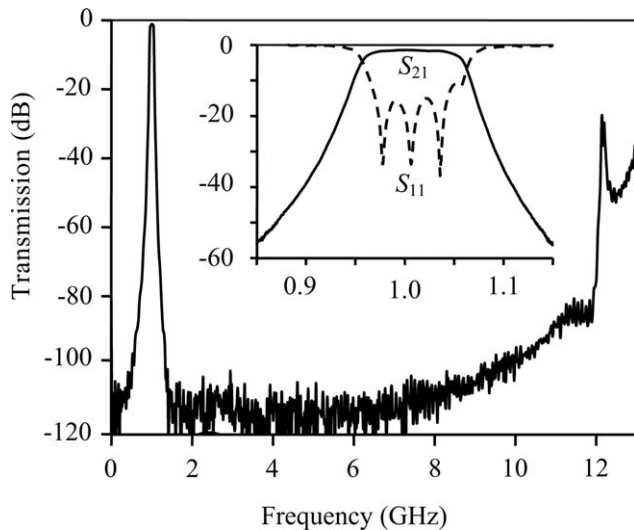


Figure 5 Measured frequency response of the suspended stripline filter

3. A FIFTH-ORDER BPF

To confirm the promising application of the proposed resonator in microwave BPFs the fifth-order filter has been designed and manufactured (Fig. 3).

The double-layer substrate of the filter was made of RT/Duroid 5880 with thickness $h_d = 0.127$ mm, permittivity $\epsilon_r = 2.2$, and dielectric loss $\text{tg}\delta \approx 0.002$. The substrate has size of 11×38 mm². All strip conductors forming the resonators have width $w = 3$ mm and length $l_s \approx 9$ mm. The air gaps have height $h_a = 3.5$ mm. The spacing between adjacent internal resonators is $S_1 = 4.5$ mm and the spacing between external and internal resonators is $S_2 = 3.75$ mm.

Figure 4 shows photograph of the fabricated filter prototype and Figure 5 shows its measured frequency response. The fabricated prototype has the passband center frequency $f_0 = 1$ GHz and the fractional bandwidth $\Delta f/f_0 \approx 10\%$ measured at the level of -3 dB. The minimum insertion loss in the passband is $L = 1.3$ dB. The filter stopband at level of -100 dB extends up to $10f_0$.

Note that the proposed BPF could have significantly smaller size if it was implemented by means of low temperature cofired ceramics (LTCC) technology. Figure 6 shows the simulated frequency response of the fifth-order monolithic filter based on materials which are in use in LTCC technology. The design parameters of the simulated filter were as follows. As material of the dielectric layers (ceramic sheets) that fills the entire volume of the filter

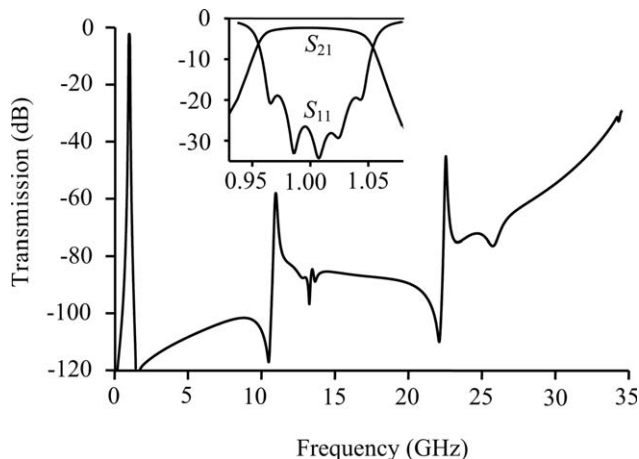


Figure 6 Simulated frequency response of the LTCC filter

TABLE 1 Simulated Stopband Characteristics of the LTCC Filter

Transmission level	-100 dB	-50 dB	-40 dB
Upper stopband edge	$10.7 f_0$	$22.7 f_0$	$33 f_0$

was chosen Heratope CT2000 ($\epsilon_r = 9.1$, $\text{tg}\delta = 0.002$). The vertical distance between the strip conductors was chosen $h_d = 20$ μm and the distance between the metal case and the outer strip conductor was chosen $h_a = 600$ μm [1]. The strip conductors were supposed to be made of cofired paste HF612 based on Ag [1]. They had width $w = 0.5$ mm, length $l_s \approx 4.0$ mm, thickness $t = 10$ μm , and surface resistivity $R_s = 2$ m Ω . The spacings between adjacent resonators were chosen $S_1 = 0.75$ mm and $S_2 = 0.625$ mm. In order to align the reflection maxima in the passband, the inner conductors of three internal resonators were shortened by length of 0.1 mm.

The simulated LTCC filter has center frequency $f_0 = 1$ GHz, fractional bandwidth $\Delta f/f_0 \approx 10\%$ measured at the level of -3 dB, and minimum insertion loss $L = 2.3$ dB. The filter has size $4.25 \times 6.25 \times 1.24$ mm³. The frequencies of the upper stopband edges measured at three different transmission levels are presented in Table 1.

One can see that the proposed suspended stripline BPFs have extremely wide and deep stopband. They are inferior only to the latest novel coaxial BPFs [10,11] but are smaller than in size and are more fabricable.

4. CONCLUSION

Thus, a novel construction of miniature stripline resonator fulfilled on a double-layer suspended substrate is proposed. This resonator differs in small size and significant difference between frequencies of high-order modes and frequency of the fundamental mode. It has rather high Q factor for so small size. It is shown experimentally that the proposed resonator is good for designing miniature BPFs with extremely wide and deep stopband. The fabricated filter has center frequency $f_0 = 1$ GHz, fractional bandwidth $\Delta f/f_0 \approx 10\%$, and minimum insertion loss $L = 1.3$ dB. Metal case of the filter has inner size of $11 \times 38 \times 7.3$ mm³. The stopband at the level of -100 dB extends up to $10f_0$. Electromagnetic 3D simulation showed that the filter manufactured with using LTCC technology may have higher performance.

ACKNOWLEDGMENTS

This work was supported by the Ministry of Education and Science of the Russian Federation under State contract No 14.513.11.0010, Federal Target Program "Research and Research-Pedagogical Personnel of Innovation Russia 2009–2013" under contracts No 16.740.11.0470, No 14.B37.21.1103, No 14.B37.21.0070, No 14.A18.21.1857, and Integration Project of Siberian Branch of the RAS No 109.

REFERENCES

1. Y.-M. Chen, S.-F. Chang, C.-C. Chang, and T.-J. Hung, Design of stepped-impedance combline bandpass filters with symmetric insertion-loss response and wide stopband range, *IEEE Trans Microwave Theory Tech* 55 (2007), 2191–2199.
2. B.A. Belyaev, S.V. Butakov, N.L. Laletin, A.A. Leksikov, V.V. Tyurnev, and O.N. Chesnokov, Selective properties of microstrip filters designed on quarter-wave codirectional hairpin resonators, *J Commun Technol Electron* 51 (2006), 20–30.
3. S.-C. Lin, P.-H. Deng, Y.-S. Lin, C.-H. Wang, and C.H. Chen, Wide-stopband microstrip bandpass filters using dissimilar quarter-wavelength stepped-impedance resonators, *IEEE Trans Microwave Theory Tech* 54 (2006), 1011–1017.
4. J.-T. Kuo and E. Shih, Microstrip stepped impedance resonator bandpass filter with an extended optimal rejection bandwidth, *IEEE Trans Microwave Theory Tech* 51 (2003), 1554–1559.

5. T.-N. Kuo, W.-C. Li, C.-H. Wang, and C.H. Chen, Wide-stopband microstrip bandpass filters using quarter-wavelength stepped-impedance resonators and bandstop embedded resonators, *IEEE Microwave Wireless Compon Lett* 18 (2008), 389–391.
6. Y.-M. Chen, S.-F. Chang, C.-C. Chang, and T.-J. Hung, Design of stepped-impedance combline bandpass filters with symmetric insertion-loss response and wide stopband range, *IEEE Trans Microwave Theory Tech* 55 (2007), 2191–2199.
7. J.-T. Kuo, S.-P. Chen, and M. Jiang, Parallel-coupled microstrip filters with over-coupled end stages for suppression of spurious responses, *IEEE Microwave Wireless Compon Lett* 13 (2003), 440–442.
8. M.Á. Sánchez-Soriano, G. Torregrosa-Penalva, and E. Bronchalo, Multipurious suppression in parallel-coupled line filters by means of coupling control, *IET Microwaves Antennas Propag* 6 (2012), 1269–1276.
9. B.A. Belyaev, N.V. Laletin, A.A. Leksikov, and A.M. Serzhantov, Peculiarities of coupling coefficients of a regular microstrip resonator, *J Commun Technol Electron* 48 (2003), 31–38.
10. B.A. Belyaev, A.M. Serzhantov, V.V. Tyurnev, and A.A. Leksikov, Miniature bandpass filter with a wide stopband up to $40f_0$, *Microwave Opt Technol Lett* 54 (2012), 1117–1118.
11. B.A. Belyaev, A.M. Serzhantov, V.V. Tyurnev, A.A. Leksikov, and A.A. Leksikov, Miniature coaxial resonator and related bandpass filter with ultra-wide stopband, *Tech Phys Lett* 38 (2012), 47–50.

© 2013 Wiley Periodicals, Inc.

PERFORMANCE OF A RECONFIGURABLE REFLECTOR ANTENNA WITH SCANNING CAPABILITY USING LOW COST PLASMA ELEMENTS

M. T. Jusoh,^{1,2} O. Lafond,¹ F. Colombel,¹ and M. Himdi¹

¹Institut d'Electronique et de Télécommunications de Rennes (IETR), Université de Rennes 1, Rennes 35042, France

²Department of Electrical and Electronics Engineering, National Defence University of Malaysia (NDUM), Kem Sungai Besi, Sungai Besi, Kuala Lumpur 57000, Malaysia; Corresponding author: taufik@upnm.edu.my

Received 13 April 2013

ABSTRACT: A reflector antenna with rounded shape is designed to collimate beam radiated by a quarter wave antenna operating at 2.4 GHz by implementing low cost plasma elements. The measured gain is 9 dBi, cross-polarization remains below -10 dB and operating bandwidth of the antenna is almost 46 percent. © 2013 Wiley Periodicals, Inc. *Microwave Opt Technol Lett* 55:2869–2874, 2013; View this article online at wileyonlinelibrary.com. DOI 10.1002/mop.27958

Key words: plasma antenna; reconfigurable antenna; beam scanning; beam shaping

1. INTRODUCTION

Plasma is the fourth state of matter with complex permittivity that can be exploited to give advantages in communication system [1]. Its negative permittivity has been studied in many research papers and it was proven to have similar characteristics as metal material in terms of electrical conductivity [2,3]. While keeping permeability in the positive region, plasma will respond to electromagnetic waves in the similar manner as metal. Therefore, plasma can be an alternative to metal in the construction of antennas. Its permittivity can be altered by changing its parameters such as plasma frequency [4,5], collision frequency [2,5], and gas density [6,7]. In Refs. 8–12, plasma encapsulated in a dielectric tube has been proven to work as a radiator. Most of the plasma tubes are homemade designed [10–12], allowing geometry of the dielectric tubes and

plasma properties to be altered. One of the earliest realization of plasma as a radiator has been carried out in [13]. Later on, G. G. Borg in [14,15] and his group have come out with experimental results for ultra high frequency and very high frequency band.

Beam shaping and beam steering by using plasma reflector are very promising profiles, especially ability of plasma to be reconfigured electrically which is impossible to be done by metal elements. Reflector antennas are simple in terms of design complexity, space, and its simple feed system where free space is used as feed network. There are several configurations of reflector antennas that can be adopted to steer incoming signal to the intended direction [16]. One of its realizations was a parabolic plasma reflector operating at 3 GHz. The reflector has shown comparable performance with metal reflector in the same arrangement [17,18]. A mathematical calculation using boundary value method was performed to predict radiation pattern of plasma antenna in circular arrangement in [19]. However, the operating frequencies used in the simulation are rationally near to the plasma frequency which could lead to imprecision, refer to [16]. Therefore, the only way to verify the results is through a concrete measurement.

To the best of our knowledge, only a few papers have reported about the scanning feasibility study of plasma reflector antennas [19], and none has reported about its verified performance except in [16]. For this reason, this article is aimed to present simulation and experimental results in order to verify the performance of the reconfigurable plasma reflector antenna with beam shaping and scanning capability operating at 2.4 GHz. The reflector elements are made of series of compact fluorescent lamps (CFL) and are arranged in circular arrangement. The implementation of CFLs has reduced the risk of complexity of impedance tuning which is vital when dealing with parasitic elements in designing antenna arrays. Each of the elements is individually controlled by a single-pole electronic switch. Therefore, to change the beam profiles is effortless by narrowing or widening plasma window. As plasma only requires microseconds to decay [20,21], the scanning beam can be manoeuvred in split seconds too. Other than antenna reconfigurability profile, reduced radar cross section [17,20], better gain, good cross-polarization, high front to back ratio, and its large operating bandwidth, the overall system is unique because it implements commercially available CFL [22] in order to stay considerably small, compact in size, and low cost, if one compares to the elements used in [16] and assumed in [19]. Comparisons between simulated and measured results in the same configuration are discussed thoroughly in this article. The simulations were run using finite-element-method-software, CST Suite [23].

2. PLASMA FORMULATION

The isotropic plasma is a dispersive material that has complex permittivity. The permittivity under low electron-neutral collision is given by Eq. (1):

$$\epsilon_r = 1 - \frac{\omega_p^2}{\omega(\omega - i\nu)} \quad (1)$$

where ϵ_r is the complex plasma permittivity, ω is the operating angular frequency [rad/s], and ν is the electron-neutral collision frequency [Hz]. The ω_p is the plasma angular frequency [rad/s], and its value can be calculated as in Eq. (2):

$$\omega_p = \left(\frac{ne^2}{m\epsilon_0} \right)^{1/2} \quad (2)$$

where n is the electron density [m^{-3}], e is the charge of electron [C], m is the electron mass [kg], and ϵ_0 is the free space permittivity [F/m]. From Eq. (1), the ϵ_r of the plasma will vary if the